Spectrochimica Acta Part A: Molecular and Biomolecular Spectroscopy 326 (2025) 125246

Contents lists available at ScienceDirect

Spectrochimica Acta Part A:
Molecular and Biomolecular Spectroscopy

journal homepage: www.journals.elsevier.com/spectrochimica-acta-part-a-molecular-and-biomolecular-spectroscopy

Investigation of the molecular interaction between apraclonidine, an α2-adrenergic receptor agonist, and bovine serum albumin using fluorescence and molecular docking techniques

Ipek Kucuk [a,b], Öykü Buket Küçükşahin [c], Merve Yildirim [b,d], Md. Zahirul Kabir [c], Hülya Silah [e,*], Ismail Celik [d,*], Bengi Uslu [c,*]

[a] Başkent University, Faculty of Pharmacy, Department of Analytical Chemistry, 06790 Etimesgut, Ankara, Turkiye
[b] Ankara University, The Graduate School of Health Sciences, 06110 Ankara, Turkiye
[c] Ankara University, Faculty of Pharmacy, Department of Analytical Chemistry, 06560 Ankara, Turkiye
[d] Erciyes University, Faculty of Pharmacy, Department of Pharmaceutical Chemistry, 38039 Kayseri, Turkiye
[e] Bilecik Seyh Edebali University, Faculty of Science, Department of Chemistry, 11210 Bilecik, Turkiye

HIGHLIGHTS

- Molecular interaction of aproclonidine–bovine serum albumin is first investigated.
- Protein fluorescence was discovered to decrease when APR bound to BSA.
- The protein's microenvironment near Tyr and Trp residues has been evaluated due to the binding of APR to BSA.
- Hydrophobic interplays, hydrogen bonds, and van der Waals forces have a notable act in the genesis of the APR–BSA complex.
- The APR binding site that was selected is located on Site II of BSA.

GRAPHICAL ABSTRACT

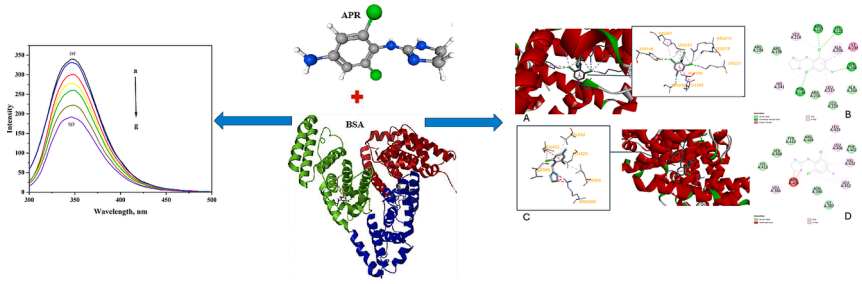

ARTICLE INFO

Keywords:
Apraclonidine
Fluorescence spectroscopy
Bovine serum albumin
Molecular docking
Ligand–protein interaction

ABSTRACT

Apraclonidine (APR) is a potent and selective α2-adrenergic receptor agonist used in the diagnosis of Horner's Syndrome, and the residuals of APR that accumulate in tissues of animals can cause central nervous and cardiovascular systems influences in humans. Therefore, to understand the influence of APR on human health, we examined the interaction of APR with the carrier protein in plasma, bovine serum albumin (BSA). The BSA fluorescence signal was quenched due to the APU–BSA complex formation and a weak binding affinity was estimated between APR and BSA. The inclusion of fluorescence, UV–vis absorption, molecular docking, and dynamics simulation techniques employed to broadly investigate the combination of APR with BSA at typical physiological conditions. The thermodynamic results revealed that enthalpy (ΔH^0) and entropy (ΔS^0) changes were computed as +11.14 kJ mol^{-1} and +97.56 J mol^{-1} K^{-1}, respectively, which represented the binding is principally entropy-driven and the hydrophobic forces acting a significant role in the reaction. Analysis of synchronous and 3-D fluorescence signals revealed microenvironmental variations close to BSA's Trp and Tyr residues upon APR addition. Both the competitive site marker as well as molecular docking results detected that APR exhibited a stronger binding affinity towards Drug Site 2 (DS2) compared to Drug Site 1 (DS1).

* Corresponding authors.
E-mail addresses: hulya.mercan@bilecik.edu.tr (H. Silah), ismailcelik@erciyes.edu.tr (I. Celik), buslu@pharmacy.ankara.edu.tr (B. Uslu).

https://doi.org/10.1016/j.saa.2024.125246
Received 21 May 2024; Received in revised form 2 September 2024; Accepted 3 October 2024
Available online 9 October 2024

1. Introduction

Apraclonidine hydrochloride (APR) is a clonidine analog that functions as an α2-agonist with an excellent level of selectivity. It is used in the diagnosis of Horner's Syndrome, which is characterized by shrinking of the pupil and drooping of the eyelid in case of paralysis of the muscles that dilate the pupil. It is widely used in the treatment of glaucoma, which causes high pressure in the eye. APR functions on the outer layer and has limited ability to penetrate the blood–brain barrier due to its composition [14]. The residuals of α-2 adrenergic agonist that aggregated in tissues of animal can cause to central nervous and cardiovascular systems influences in humans, with the inclusion of health problems such as tachycardia, dizziness, muscle tremors, and palpitations [11,8]. The chemical name for APR is 2-[(4-amino-2,6 dichloro phenyl)imino] imidazolidine monohydrochloride (as shown in Fig. 1) with a molecular weight of 281.6 Da.

Previous studies have shown that drug-protein interactions in the circulation may significantly affect the free concentration, delivery, and metabolism of several medicines [6]. The binding of the diverse drug molecules to serum albumins, generally, is a necessary study to identify the drug's potential pharmacodynamic and pharmacokinetics profile of drug molecules [2]. Thus, the research of the interplays between proteins from serum and other chemicals have significant therapeutic importance. These proteins are categorized in three major groups viz., fibrinogen, albumin, and globulin [33]. The preservation of blood pH and management of blood permeability are crucial roles performed by albumins. In the bloodstream, serum albumins are the predominant proteins, and their primary physiological role is to facilitate the transportation of various ligands to their respective organs of focus. Given its role as a messenger protein, serum albumin has often been utilized as a paradigm for investigating protein–drug interactions and binding processes [31,23,9,30]. The reason why bovine serum albumin (BSA) is one of the most investigated proteins is primarily owing to its high homology (about 76 %) and analogous 3D structure to human serum albumin (HSA) [51,36]. Also, BSA has been investigated widely in affinity and kinetic drug experiments as a replacement for HSA in consequence of its simple availability, high stability, and capability to bind diverse ligands [53]. In this respect, we have selected BSA as model protein for our research.

Spectral techniques are a vigorous apparatus to explain the binding of molecules such as drugs with albumin proteins at low concentrations. One of the straightforward techniques that is generally utilized to survey protein conformational alterations upon interactions with diverse molecules is fluorescence spectroscopy due to its perfect selectivity, sensitivity, and theoretical bases. The intrinsic BSA fluorescence is because of the existence of its aromatic amino acid residuals with the inclusion of tryptophan (Trp), tyrosine (Tyr), and phenylalanine (Phe) [31,24]. BSA owns three main ligand-drug binding sites I, II, and III located in subdomain IIA, IIIA, and IB, respectively. This protein is composed of two Trp residues, Trp-212 (in the hydrophobic space) and Trp-134 (existent on the surface), liable for its intrinsic fluorescence feature [19].

Taking into consideration of significance of APR under investigation and the importance of drug binding to plasma proteins also owing to deficiency of literature on the binding mechanism of APR with BSA, we are interested to survey its interaction with BSA by determining its binding factors such as mode of binding, binding constants, number of binding sites, thermodynamic properties, protein's microenvironmental changes and binding location. The exploration of APR–BSA interaction was made utilizing fluorescence, UV–Vis absorption, molecular docking, and molecular dynamics simulation procedures.

2. Materials and methods

2.1. Reagents and experimental solutions

Analytical grade of BSA (originally protease, fatty acid, and globulin free), APR, indomethacin (IDM) and, ibuprofen (IBU) were purchased by Sigma-Aldrich Corporation, USA. The buffer used in all experiments to simulate extracellular physiological conditions was 60 mM sodium phosphate with a pH of 7.4 (PBS 7.4). Stock solution of BSA was made in PBS 7.4 and concentration of BSA was ascertained spectrophotometrically handling the molar extinction coefficient as $\varepsilon_m = 43\,824\ M^{-1}\ cm^{-1}$ at 280 nm. Stock solutions are prepared by dissolving 1 mg/ml of APR in ultrapure water, dissolving IBU and IDM in ethanol, and then diluting them in PBS 7.4 to get the necessary concentrations for experimental procedures.

2.2. UV–vis absorption spectral measurements

With a conventional quartz cuvette with a 1 cm optical path length, the spectral measurements were performed using a Shimadzu 1601PC double beam UV–vis absorption spectrophotometer. The absorption spectra (λ = 280–500 nm) of 3 μM BSA solutions with and without increasing APR concentrations (ranging from 50–350 μM with intervals of 50 μM) were collected for the inner filter effect correction in the fluorescence data. The absorption spectra (λ = 240–320 nm) of 20 μM BSA with increasing APR concentrations (0–350 μM with 50 μM increments) were also recorded in a separate experiment.

2.3. Fluorescence spectral measurements

The fluorescence spectra of BSA and APR–BSA system were recorded on an Agilent Cary Eclipse spectrophotometer using 1 cm quartz cuvette, placed in a Peltier type thermostat cell holder attached with a water bath cyclical. The 3 μM BSA fluorescence signals (λ_{em} = 300–500 nm) without and with addition of APR (50–350 μM with intervals of 50 μM) were registered using the λ_{ex} of 280 nm. Before fluorescence spectrum scans, the solution mixtures (3 ml) for titration investigations were singly stayed at various temperatures as 288, 298, and 308 K for a period of 30 min in order to arrive equilibrium.

Synchronous fluorescence spectra of BSA (3 μM) were recorded with rising concentrations of APR (between 0 and 350 μM with intervals of 50 μM), by assaying Δλ = 15 nm and Δλ = 60 nm for Tyr and Trp residues in the wavelength range of 250–350 nm and 240–400 nm, respectively.

Three-dimensional (3-D) fluorescence spectra were measured to

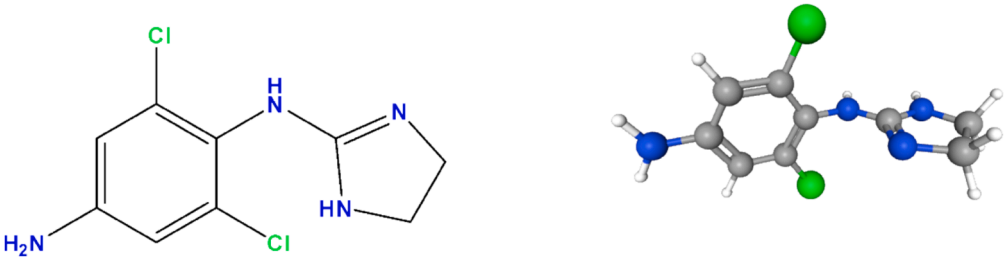

Fig. 1. The 2-D and 3-D structures of APR.

analyze alterations in the biochemical environment of Trp and Tyr residues, which serve as protein fluorophores. This was done using BSA at a concentration of 3 μM and a 50:1 APR-BSA combination at a temperature of 298 K. The excitation wavelength (λ_{ex}) range was 220–350 nm with a sampling interval of 5 nm, and the emission wavelength (λ_{em}) range was 220–550 nm.

2.4. Analysis of APR–BSA fluorescence enhancement data

The fluorescence titration data for the APR–BSA interaction were setted to avoid the inner-filter influences utilizing the following equation (Eq. (1)):

$$F_{corr} = F_{obs} 10^{\frac{(A_{em}+A_{ex})}{2}} \quad (1)$$

where F_{cor} and F_{obs} were the corrected fluorescence intensities and observed fluorescence intensities, respectively; A_{em} and A_{ex} were the absorbance value of APR–BSA complex and BSA at the emission and excitation wavelengths, respectively.

To identify the fluorescence quenching mechanism and binding affinity in the APR–BSA binding process, the Stern–Volmer equation and double logarithmic equations were utilized (Eqs. (2) and (3)), respectively. After the linear regression analysis, the fluorescence quenching data at diverse temperatures (288 K, 298 K and 308 K) were implemented a statistical analysis.

$$\frac{F_0}{F} = 1 + K_{sv}[Q] = 1 + K_q \tau_0 [Q] \quad (2)$$

$$log\left[\frac{F - F_0}{F}\right] = nlogK_a + nlog[Q] \quad (3)$$

In these equations, F_0 and F represent the fluorescence intensities of BSA in nonexistence and in existence of quencher, respectively. τ_0 is the mean lifetime of the fluorescent molecule without the quencher and the fluorescence lifetime of macromolecules like BSA is usually valued 5.6×10^{-9} s. The term Q is the concentration of quencher (APR). The Stern–Volmer quenching constant (K_{sv}), bimolecular quenching rate constant (k_q), number of binding sites (n) and binding constant (K_a) values were retrieved from these equations [44,45,48,17].

The binding forces comprised in the APR–BSA interaction were furthermore defined with the assistance of the thermodynamic parameters using enthalpy change (ΔH^0), entropy change (ΔS^0), and free energy change (ΔG^0). These parameters were calculated using the following equations (Eqs. (4) and (5)) [13].

$$lnK_a = -\frac{\Delta H}{RT} + \frac{\Delta S}{R} \quad (4)$$

$$\Delta G = \Delta H - T\Delta S \quad (5)$$

2.5. Ligand displacement measurements

The binding location of APR on BSA was determined by the use of two markers uniquely present at that site: IDM (Site I) and IBU (Site II). Titrations of 3 μM BSA and 1:1 IDM–BSA/IBU–BSA (previously incubated at 298 K for 30 mins) mixes with adding APR (50–350 μM with 50 μM intervals) were conducted upon the λ_{ex} at 280 nm, after subsequent incubation of these samples at 298 K for 30 min.

2.6. Molecular docking study

The crystal structure of BSA in complex with 3,5-diiodosalicylic acid (PDB ID: 4JK4) [39] was obtained from the RCSB Protein Data Bank. The BSA structure was processed using Discovery Studio Visualizer v21.1.0, which involved removing all ligands and water molecules. Subsequent modifications included the addition of polar hydrogens and the assignment of Kollman charges to prepare the protein for docking. The chemical structure of APR was retrieved from PubChem (PubChem CID: 2216). To prepare the ligand for docking, energy minimization was performed using Chimera version 1.17.3. The molecular docking study was conducted using DiffDock, an advanced application recently developed for this purpose. DiffDock employs a generative artificial intelligence algorithm that predicts the optimal pocket for ligand docking based on learned calculations from previous steps. This algorithm is notable for its rapid inference capabilities and for providing confidence estimates with high selective accuracy. After conducting the molecular docking, DiffDock provided a ranking of potential docking poses. Discovery Studio Visualizer displayed the two poses that achieved the highest molecular docking scores, highlighting the optimal interactions between the ligand and the protein target.

2.7. Molecular dynamic simulation study

Molecular dynamics (MD) simulations of the protein–ligand complex involving APR and BSA's DS1 and DS2 regions were initiated using input files prepared with the default settings of the Solution Builder on the CubeBuilder 1.5.1 server. Topology files for both the protein and the ligand were generated using the Amber ff99SB force fields [28]. The MD simulations were conducted using Gromacs version 2023.3 over a period of 150 ns, capturing a total of 1500 frames. The MD simulation cubic box included 0.15 M KCl and utilized the OPC water model, simulating physiological conditions accurately 10 Å away from protein ligand. The molecular dynamics employed the MD integration method with a time step of 0.002 picoseconds. Non-bonded interactions were managed using a Verlet list for the cutoff scheme, updated every 20 steps. Van der Waals forces were handled with a cutoff method, and electrostatic interactions were processed using the Particle Mesh Ewald (PME) method. The system's temperature was maintained at 310 K using the Nose-Hoover thermostat, and pressure was controlled at 1.0 bar using the Parrinello-Rahman barostat, ensuring consistent thermodynamic conditions. To specifically analyze the stability of APR with BSA's DS1 and DS2 regions, the simulations focused on monitoring interactions and binding efficiencies between the ligand and these protein domains. Root mean square deviation (RMSD) and root mean square fluctuation (RMSF) analyses were performed to assess the overall stability and flexibility of the complex. Principal component analysis (PCA) was employed to understand the dominant motion patterns, and hydrogen bond analysis provided insights into the critical interactions within the complex. Dynamic visualization of the interactions between APR and BSA's domains was achieved through molecular dynamics animation videos created using PyMOL v2.4.

3. Results and discussion

3.1. Analysis of APR binding to BSA

3.1.1. BSA fluorescence quenching upon APR binding

Spectral techniques are a vigorous apparatus to explain the binding of molecules such as drugs with albumin proteins at low concentrations. These binding affinities of proteins can be identified by fluorescence quenching technique. Such a reducing in the fluorescence efficiency in the existence of a quencher is named fluorescence quenching. Fluorescence technique is utilized to observe molecular interactions, due to its high reproducibility, sensitivity, and relatively effortlessness of operate [50]. Fluorescence spectroscopy is employed to research molecule-protein binding mechanisms to acquire knowledge on the number of binding sites, binding constant, and thermodynamic variables [12]. The inimitable capability of proteins to demonstrate intrinsic fluorescence has ensured a pathway to comprehension of the alterations in its environment upon quencher interplay [41]. The intrinsic fluorescence of BSA is principally by virtue of Trp residues, because Phe has a very low quantum efficiency and the fluorescence of Tyr is nearly completely quenched if it is ionized or near a carboxyl or amino group, or a

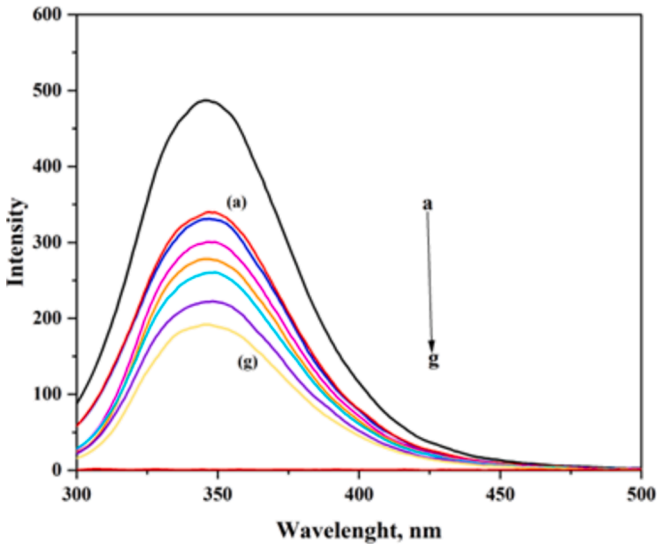

Fig. 2. Fluorescence emission spectra of APR–BSA system obtained in the nonexistence and presence of APR. [BSA] = 3 μM and [APR] = (a) 50 μM (b) 100 μM (c) 150 μM (d) 200 μM (e) 250 μM (f) 300 μM (g) 350 μM.

resonance energy transference can be formed from Trp or Tyr residues [15,27]. When BSA is stimulated by convenient wavelengths of electromagnetic light, all of its fluorophores (Phe, Trp, Tyr) can radiate fluorescence. When a 280-nm stimulation wavelength is utilized, the fluorescence of albumin stems from both Tyr and Trp residuals, however a 293-nm wavelength only excites Trp residual [26,43].

The alteration in the fluorescence spectra of BSA with consecutive additions of APR using the λex of 280 nm at 298 K were shown in Fig. 2. It is monitored that BSA has a powerful fluorescence emission signal at 347 nm after being excited. When the concentration of APR was increased, the intensity of the strong emission band of BSA fluorescence at 347 nm decreased significantly. It can be understood that the fluorescence intensity of BSA was effectually quenched when the concentrations of APR raises, pointing out an interaction between APR and BSA.

3.1.2. Quenching mechanism analysis

The occurred quenching may be the ensues of molecular interactions such as collisions, energy transfer reaction, rearrangements, and formation of complex in ground state or excited state (Jalan and Moyon, 2024). However, the mechanism of fluorescence quenching is generally classified as static quenching (ground-state complex generation) and dynamic quenching (molecular collision), which can be diversified by temperature dependency. In the static quenching process, ascending temperature decreases the stability of quencher-fluorophore complex, ensuing in a lower quenching constant. But, in dynamic quenching, the quenching constant will increase with increasing temperature because of the greater collision and diffusion of the fluorophore and quencher [29,32,45].

To identify the fluorescence quenching mechanism in the APR–BSA binding process, the Stern–Volmer graphs (Fig. 3) were prepared by analyzing the fluorescence quenching data of APR–BSA system obtained at 288, 298 and 308 K using Eq. (2). For the APR–BSA system, the relation between F_0/F and APR concentrations had a better linear. The experimental results brought to light that the values of K_{sv} increased from 1.12×10^5 to 1.57×10^5 L·mol^{-1}·s^{-1} while the temperature was steadily raised. According to the K_{sv} values in Table 1, it can be said that the probable mechanism of fluorescence quenching of BSA in the existence of APR is a dynamic quenching process related to K_{sv} value increment with increasing the temperature from 288 to 308 K.

In dynamic quenching process, high temperature values cause more quick dissemination steady and make progress electron transfer, and for this reason, K_{sv} inclines to increment [49,5]. Also, the K_q values also increased when the temperature rising and these values at 288–308 K were faraway in excess of the maximum dynamic K_q of 2.0×10^{10} L·mol^{-1}·s^{-1}. It is disclosed that APR quenches the fluorescence of BSA in the form of a static quenching. So, it can be brought to a result that APR quenched fluorescence intensity of BSA via hybrid quenching mechanism [21,40].

3.1.3. Absorption spectral analysis

UV–Vis spectroscopy is a valuable method for confirming the quenching process and evaluating the creation of ligand–protein complexes. The protein's absorption spectrum perturbations are often caused by static processes. However, the absorption spectra of the protein remains unchanged due to dynamic quenching, which only affects the excited state of the fluorophore. It was seen that the BSA absorption spectra displayed hyperchromaticity at about 280 nm upon increasing

Table 1
APR-BSA interaction and thermodynamic parameters at different temperatures.

T (K)	K_{sv} (M^{-1})	k_q (M^{-1} s^{-1})	K_a (M^{-1})	n	ΔS (J mol^{-1} K^{-1})	ΔH (kJ mol^{-1})	ΔG (kJ mol^{-1})
288	1.12×10^5	2.00×10^{13}	1.18×10^3	0.88	+97.56	+11.14	−16.94
298	1.34×10^5	2.40×10^{13}	1.42×10^3	1.26			−17.98
308	1.57×10^5	2.80×10^{13}	1.59×10^3	0.87			−18.88

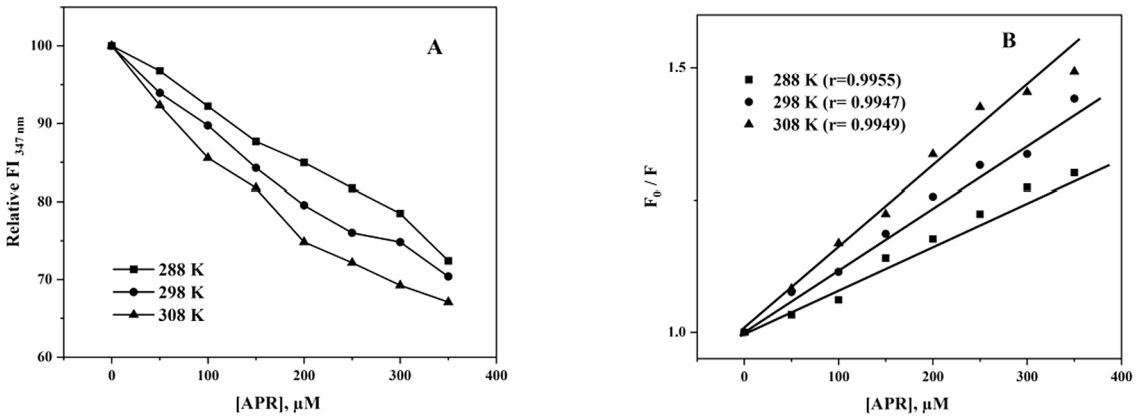

Fig. 3. (A) At three different temperatures, the fluorescence signals at 347 nm of BSA decrease as the concentrations of APR rise, and (B) at the specific temperature, the interaction between APR and BSA is shown by linear Stern-Volmer plots.

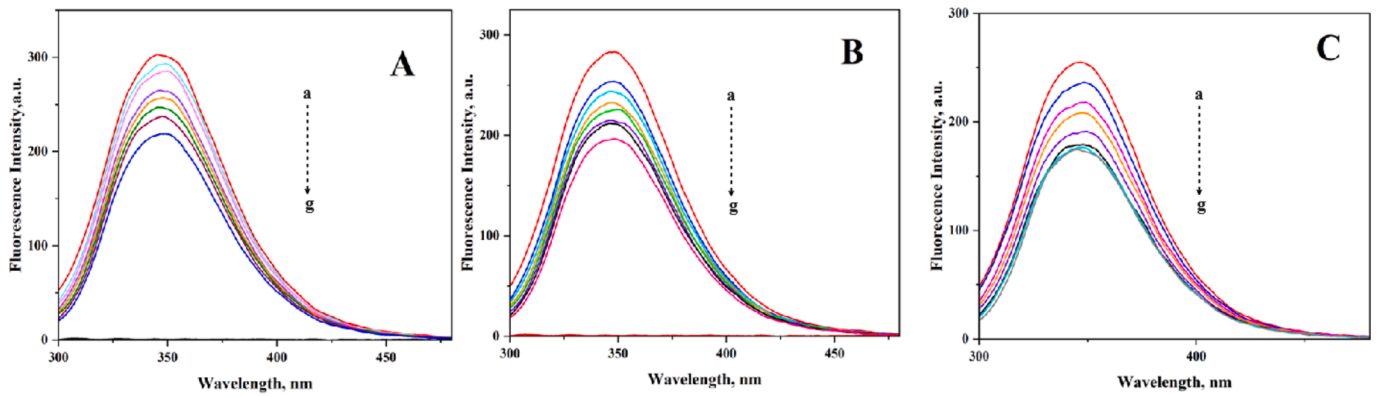

Fig. 4. BSA fluorescence emission spectra in the existence of various APR concentrations in three different temperatures. (A) T = 288 K, (B) T = 298 K and (C) T = 308 K. [BSA] = 3.0 μM, [APR] = 0–350 μM (spectra a-g). pH = 7.4 PBS. λex = 280 nm.

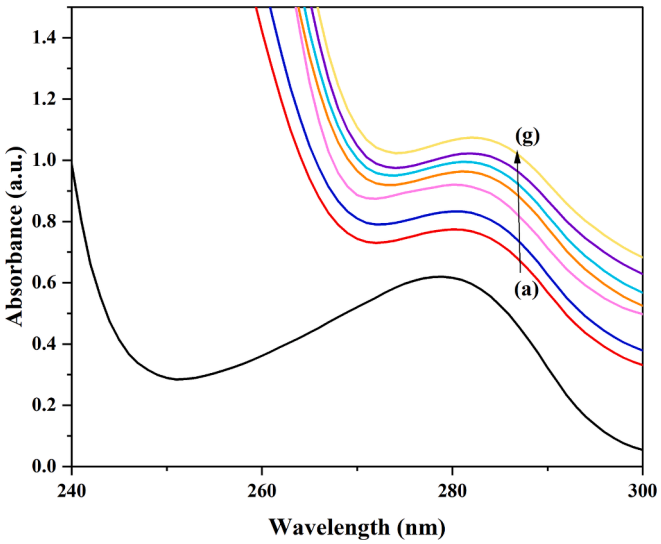

Fig. 5. Ultraviolet–visible absorption spectra of BSA without and with increasing concentrations of APR. Experimental conditions: [BSA] = 20 μM; (a) 50 μM (b) 100 μM (c) 150 μM (d) 200 μM (e) 250 μM (f) 300 μM (g) 350 μM.

concentrations of APR [34,10]. It can be concluded with confidence that the quenching of APR to BSA is a static process, resulting in the formation of ground state APR–BSA complex (Fig. 5). The findings mentioned above align with the results obtained from our fluorescence spectroscopic analysis.

3.1.4. *Binding constants and binding points*

If small molecules such as APR interact one by one with a set of equivalent sites on macromolecules such as BSA, the probable binding constant (K_a) and number of binding site (n) of APR–BSA can be investigated by the intercept and slop of the double logarithmic plots at different temperatures using Eq. (3) [5].

A plot between $\log[(F_0 - F)/F]$ versus log[Q] (Fig. 6) was employed to calculate the n and K_a values using the data obtained from Fig. 5, are included in Table 1. Over the investigated temperature range, the number of binding sites (n) was unity, recommending that only one kind of binding site was existent on BSA that could bind to APR. K_a defines the extent of distribution of drug in human plasma, and a higher K_a value displays a powerful binding interaction between the ligand and protein. In this study, the values of K_a for APR–BSA interaction were calculated as be in the scale of 1.18–1.59 × 10^3 M^{-1} indicates that a weak binding affinity between APR and BSA. The K_a values displayed a rise in binding strength with increasing temperatures in interplay of APR and BSA implied the loss of strength in the complex formation at higher temperature [49]; (Moghaddam et al., 2014); [48,25]; (Jattinagoudar et al., 2017).

3.1.5. *Thermodynamics parameters and nature of the binding forces*

Diversified non-covalent interactions behave as driving forces in protein-drug interactions. These forces are hydrophobic forces, van der Waals interactions, electrostatic interactions, and hydrogen bond formation. The forces behaving between a protein and drug molecule can be defined with the assist of thermodynamic properties such as enthalpy change (ΔH°), free energy change (ΔG°), and entropy change (ΔS°) [1,46,33]. When the reports in the literature about ligand–protein interactions are examined, magnitude and sign of the various

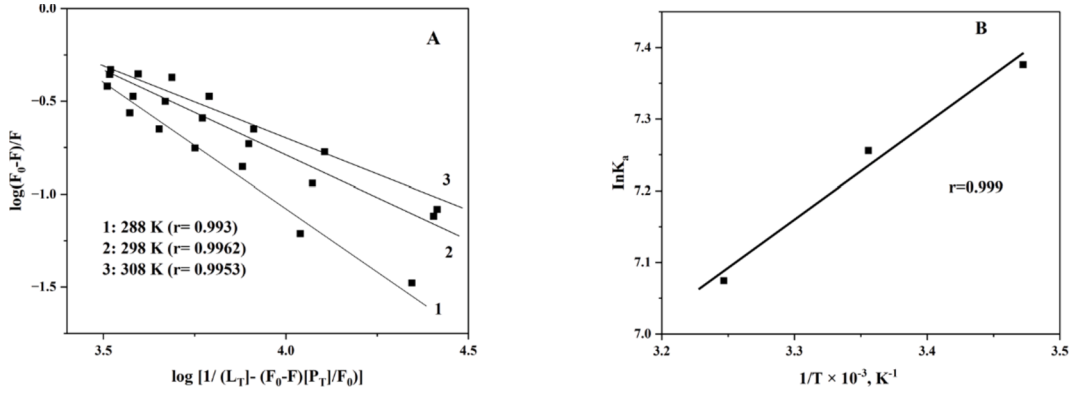

Fig. 6. (A) Double logarithmic and (B) Van't Hoff plots for the APR–BSA interaction at three temperatures 288, 298, and 308 K, as acquired from the data given in Fig. 4.

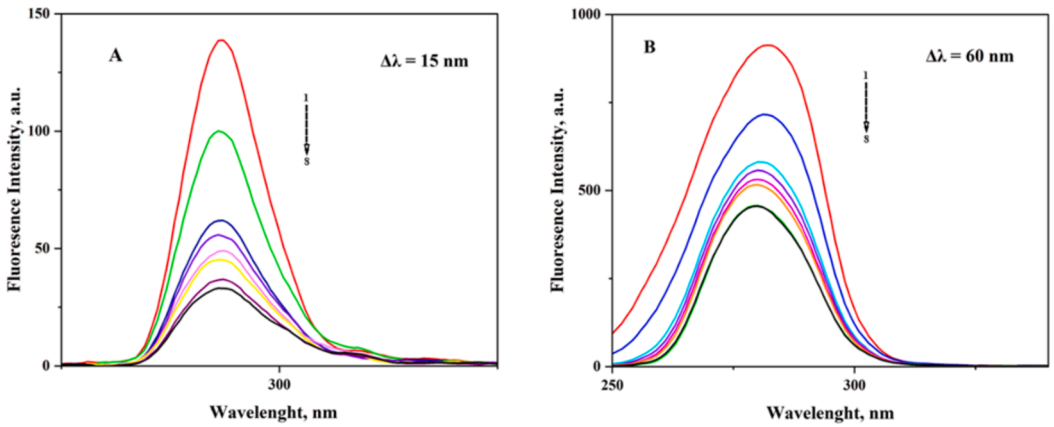

Fig. 7. The synchronous fluorescence signals of 3 μM BSA show a decrease in fluorescence intensities as the concentrations of APR increase. The spectra '1–8′ demonstrate this trend, with APR concentrations ranging from 0 to 350 μM in 50 μM intervals. The recordings were made using Δλ = 15 nm and 60 nm. Experimental conditions: the buffer used was PBS with a pH of 7.4, and the temperature was maintained at 298 K.

thermodynamic properties relating to the varied kinds of ligand–protein interactions demonstrates that van der Waals forces and hydrogen bonding result in negative ΔS^0 and ΔH^0 values. A hydrophobic interaction is coherent with positive ΔS^0 and ΔH^0 of a system, whereas, negative ΔH and positive ΔS correspond to electrostatic interactions [2,37,38]. Therefore, the ΔS, ΔH and ΔG values for APR–BSA interaction were obtained from the van't Hoff plot (insert of Fig. 4) and Eq. (5) to confirm the association of intermolecular forces in the binding process. All these values are summarized in Table 1. The values of ΔG, ΔS, and ΔH for APR–BSA interaction were acquired from the van't Hoff plot (Fig. 6B) and Eqs. (4) and (5), and are given in Table 1. For APR–BSA system, the ΔH and the ΔS values are positive, and the ΔG value is negative at all three temperatures. The negative value of ΔG means that APR binding to BSA is spontaneous. Additionally, according to the precepts summarized by Ross and Subramanyam, for drug molecule–protein interaction, the calculated positive ΔH and ΔS values of the interaction between APR and BSA indicated that the binding is principally entropy-driven, and the enthalpy is endothermic nature for the system, the hydrophobic forces acting a significant role in the reaction [16,37].

3.2. Conformational studies

3.2.1. Synchronous fluorescence results of APR-BSA interaction

The synchronous fluorescence spectrophotometric studies were enforced to acquire knowledge concerning the microenvironmental changes surrounding protein fluorophores brought on by binding of drug molecules [49]. Synchronous fluorescence method supplies knowledge on the molecular environment in the vicinity of the fluorophores of serum albumins. Also, knowledge of changes in the fluorescing aromatic residues can be obtained from the synchronous fluorescence spectra. This fluorescence method has some superiorities including spectral facilitation, band width reduction and for this reason a reducing of the results that interfere in the steady-state method [42,52,30]. Synchronous fluorescence method comprises the synchronous scanning of excitation and the fluorescence monochromators of a fluorometer, while keeping a stationary wavelength difference between them [18]. In this study, synchronous fluorescence spectroscopy was utilized to ascertain if the alterations that take place in the microenvironment of Trp or Tyr residuals because of their interaction with APR are identical or distinct. The fluorescence that occurs simultaneously in the Tyr and Trp residues offers separate knowledge on the alterations in polarity that occur surrounding them when the Δλ was selected at 15 nm and 60 nm, respectively. At minor values of Δλ, the synchronous fluorescence of a Tyr/Trp mixture is peculiar of Tyr (15 nm), however at large Δλ value the spectra is alike to that of Trp (60 nm) [20]. Fig. 7A and B demonstrates the synchronous spectra of BSA before and after binding with APR at Δλ = 15 and 60 nm with varying concentrations of APR (0–350 μM).

It is obvious from Fig. 7 that the fluorescence intensities of both Tyr and Trp were reduced with increasing concentrations of APR. When Δλ was 15 nm, the emission maximum of Tyr residues does not represent considerable shift, which pointed out that interaction of APR with BSA does not assume the conformation of the Tyr microenvironment [7]. It is

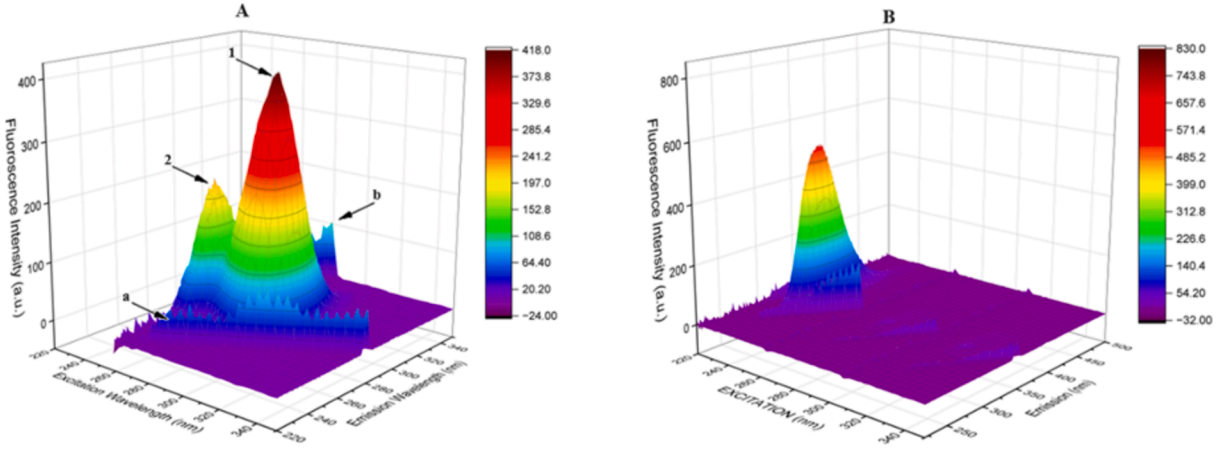

Fig. 8. 3D fluorescence spectra of (A) 3 μM BSA and (B) 50:1 APR-BSA mixture at 298 K and pH 7.4.

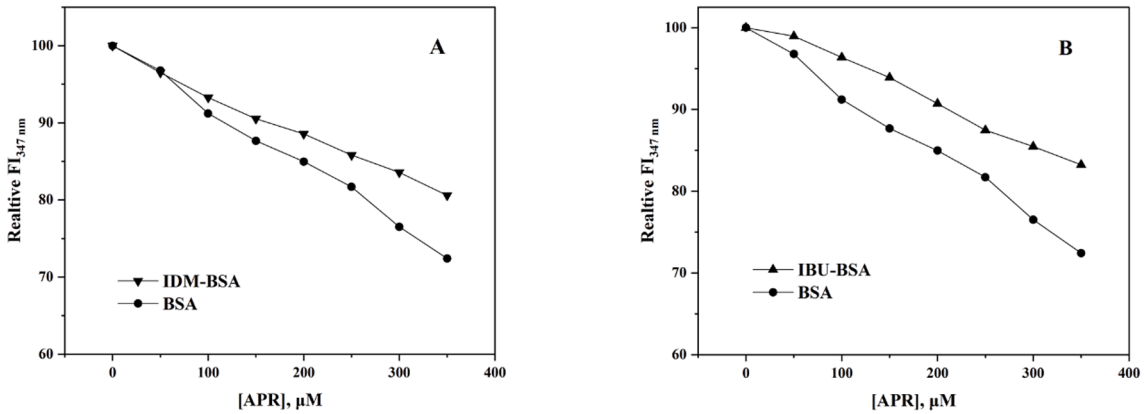

Fig. 9. Competitive displacement of site-specific marker ligands bound to BSA in the presence of increasing APR concentrations as studied by fluorescence intensity measurements. Plots showing the decrease in the relative FI_{347} nm of BSA (3 μM) and its complexes (1:1) with (A) IDM and (B) IBU with increasing concentrations of APR (50–350 μM). Experimental conditions; buffer = PBS 7.4; T = 298 K.

obvious from Fig. 7B that the emission maxima of Trp residue had blue shift which states the alteration in conformation of BSA; the polarity around the Trp residue declines and hydrophobicity rises (Yu et al., 2011, [3]. The above results hinted that microenvironmental changes near the Trp residue in BSA were conveyed by the binding ARP to BSA.

3.2.2. *Three-dimensional fluorescence results of APR–BSA interaction*

Because of the simultaneous monitoring of excitation and emission wavelength also fluorescence intensity, 3-D fluorescence spectra are getting attention [4]. So, 3D fluorescence spectroscopy technique is an important strong technique for investigating conformational alterations of proteins. The impacts of drug molecules on secondary structure of BSA and microenvironment of amino acid can be defined by comparing the relation signals for BSA fluorescence intensity with λ_{ex} and λ_{em} wavelength before and after drug binding. The results of 3D fluorescence spectral of BSA and APR–BSA mixture are given in Fig. 8.

The 3D fluorescence spectra of APR and APR–BSA were dissimilar, which remarked that there were significant interactions between APR and BSA. The results displayed that there were four emission bands (marked as Peaks 'a', 'b', '1' and '2') for BSA solution. Peaks 'a' and 'b' were the first order (because of $\lambda_{ex} = \lambda_{em}$) and the second order (because of $2\lambda_{ex} = \lambda_{em}$) Rayleigh scattering peaks, respectively. Two other strong peaks, '1' and '2' commonly reflected the fluorescence spectral behaviors of the protein's Trp and Tyr residues [40]. As shown in Fig. 8, the fluorescence intensity of Peak '1′ apparently reduced after the addition of APR. However, the fluorescence intensity of Peak '2' improved when APR was added to BSA solution, representing the diameter of macromolecule rised [35,47]. These results verified that the existence of APR transformed the microenvironment around fluorophores of BSA, consequently promoting the APR–BSA complexation. The findings were coherent with that obtained from synchronous fluorescence spectra data.

3.2.2.1. Competitive drug displacement result. There are primary binding

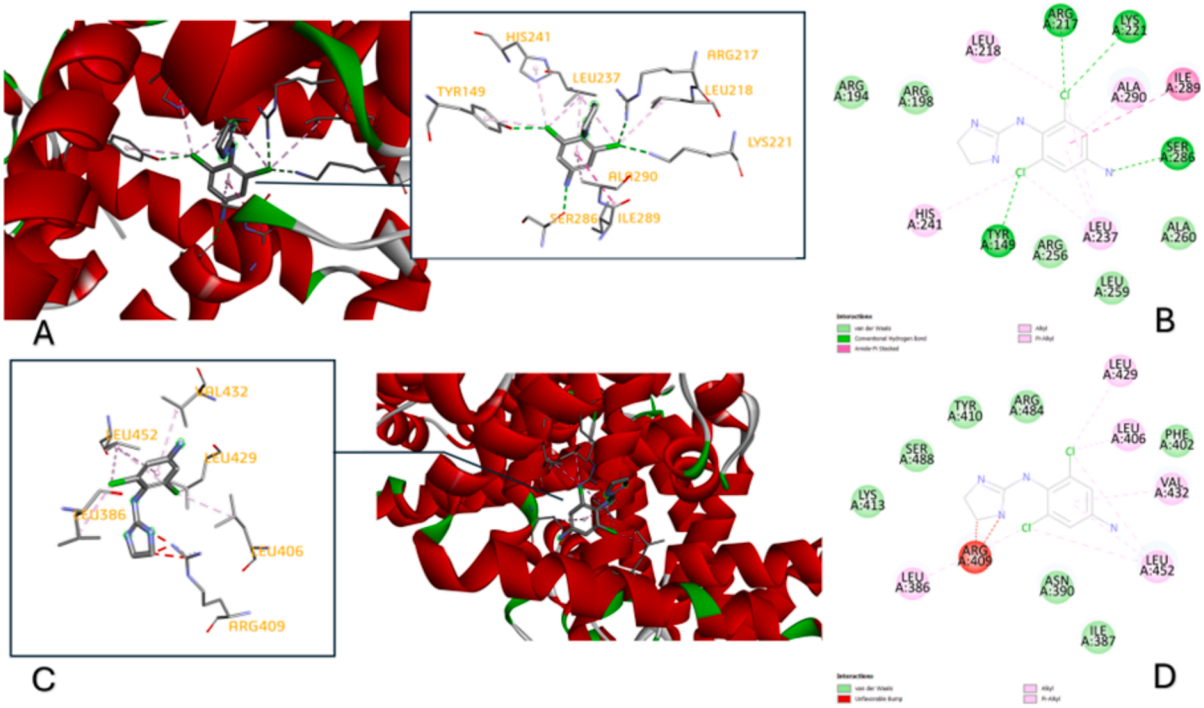

Fig. 10. 2D and 3D interactions of the APR in DS1-2 of BSA **(A and B)** 3D and 2D interaction demonstration of APR in DS1 **(C and D)** 3D and 2D interaction demonstration of APR in DS2.

Table 2
Interacting bonds and their lengths between BSA (DS1-DS2) and APR.

Binding sites	Protein-ligan interaction types		
	H-bond	Hydrophobic interactions	Van der Waals
DS1	Arg217 (3.23 Å), Lys221 (3.20 Å), Tyr149 (2.74 Å), Ser286 (3.31 Å)	Leu218 (5.08 Å), Ala290 (4.39 Å), Ile289 (4.84 Å), Leu237 (5.19–4.84–4.63 Å), His241 (4.43 Å)	Ala260, Leu259, Arg194-198–256
DS2	–	Leu429 (3.61 Å), Leu406 (4.14 Å), Val432(4.75 Å), Leu452 (5.21–5.11–4.80 Å), Leu386 (4.17 Å)	Lys413, Ser488, Tyr410, Arg484, Phe402, Asn390, Ile387, Arg409

sites, known as sites I and II, located in subdomains IIA and IIIA, respectively, within the hydrophobic cavity of BSA. Site-specific markers like IDM (for site I) and IBU (for site II) are commonly used to detect the binding sites of molecules on BSA [23,22]. To determine the desired APR binding site in BSA, we conducted titrations of the 1:1 IDM–BSA and IBU–BSA complexes with progressively higher levels of APR. Fig. 9A and B show the titration results of BSA and IDM–BSA / IBU–BSA complexes as the APR concentrations rise. Investigations of the variations in fluorescence intensity values between unbound BSA and BSA bound to the marker suggest a possible competition between two substances. Our results showed a regular decrease in the fluorescence signals with rising APR concentrations for BSA and IDM-BSA/IBU-BSA mixtures. Although, the reduce was considerably higher for IDM–BSA mixture than pure BSA and IBU–BSA complex, indicated that site II was detected as the preferably chosen APR binding site on BSA. The molecular docking analysis provided strong support for our competitive displacement results, as we will discuss later.

3.2.3. *Molecular docking results*

In order to approve the experimental knowledge, molecular modeling studies were performed. Molecular docking is a beneficial simulation that evaluates the estimation of optimum binding modes and the showing of possible interactions between target proteins and potential medicinal molecules [12].

In this study, molecular docking was utilized to predict how a ligand and a protein-bound based on their three-dimensional structures. This computational technique assigned scores to each interaction, ranking the ligands according to their docking affinity. For this study, the top-scoring interactions were analyzed to elucidate the binding mechanisms between APR and the BSA protein. Detailed visual representations, including 2D and 3D binding patterns, were generated to depict the bonds and distances involved in these interactions.

In this study, molecular docking was performed on the complexes formed by BSA and APR. Fig. 10 illustrates the 2D and 3D interactions of the APR molecule at drug binding site 1 (DS1) and binding site 2 (DS2) of BSA. According to the molecular docking analysis, APR exhibited a stronger binding affinity towards DS2 compared to DS1. The APR-BSA complex at DS1 demonstrated interactions such as van der Waals, conventional hydrogen bonds, alkyl, π-alkyl, and amide-π stacked bonds. In contrast, DS2 predominantly featured alkyl, π-alkyl, and van der Waals interactions, as detailed in Table 2. Notably, the chlorine atoms of APR and the amino acid residues Arg217 (3.23 Å), Lys221 (3.20 Å), and Tyr149 (2.74 Å) engaged in conventional hydrogen bonding, underscoring critical points of interaction that may influence the binding stability and specificity.

3.2.4. *Molecular dynamics simulation results*

Molecular dynamics simulations were utilized to analyze the behavior of proteins and ligands at the atomic level. These simulations, offering precise temporal resolution, predicted the behavior of each atom within a protein and its associated ligand over time, based on established physics models. This approach enabled observations of whether the interactions between the ligand and protein were stable within the active pocket. In this study, the dynamics of APR with DS1 and DS2 were monitored over a period of 150 ns, observing the molecule's stability within these regions. Molecular dynamics simulations allow for the interpretation of various parameters, such as RMSD, RMSF, hydrogen bond counts, and PCA data. Molecular dynamics simulation trajectory analysis is given in Fig. 11. The RMSD analysis indicated that the complexes in both DS1 and DS2 stabilized at around 0.5 nm, suggesting a robust interaction within the active sites (Fig. 11A). RMSF analysis revealed that APR's mobility was lower in DS1 compared to DS2, indicating greater stability at DS1 (Fig. 11D). This is particularly

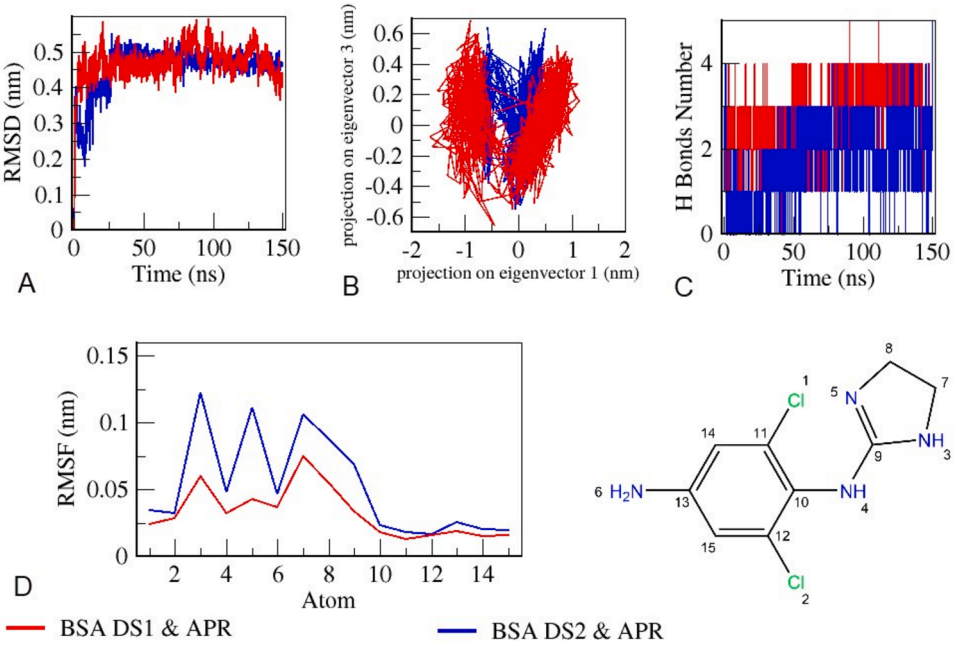

Fig. 11. The graphical data was obtained from molecular dynamics simulation. (**A**) RMSD indicated the stability of the ligand in the protein, (**B**) the similarity of the 2D projections on the eigenvectors indicated the similarity of the motions, (**C**) the number of H-bonds was an important parameter for the interaction and stability of the molecule and protein, and (**D**) RMSF showed how flexible each atom.

significant as it suggests that despite DS1′s higher dispersion as shown in PCA data, its interaction with the ligand remains more stable. Hydrogen bond analysis showed that the number of hydrogen bonds typically ranged between three to four for DS1 and two to three for DS2, indicating strong interactions within the active sites (Fig. 11C). PCA was employed to analyze large-scale motions within the protein structure. By calculating eigenvectors from the covariance matrix of the simulation and analyzing trajectories along these vectors, dominant motions during the simulation were identified. Despite DS1′s greater molecular mobility and flexibility, the lower RMSF values for APR in DS1 indicate a higher level of stability compared to DS2 (Fig. 11B). Finally, Supporting Information Videos S1 and S2, resulting from the MD simulations, showed that APR remained stable in both binding sites.

4. Conclusion

In this study, the binding mode, binding sites, binding constants, significant forces, and structural alterations of BSA in the process of binding with APR were examined by spectroscopic techniques and computational investigations. The values of Ka ($1.18–1.59 \times 10^3\ M^{-1}$) proposed a weak binding strength between APR and BSA. The acquired results indicated that the mechanism of fluorescence quenching of BSA by APR is a combination of both dynamic and static quenching process. The thermodynamic results revealed that, positive ΔH^0 and positive ΔS^0 represented that the binding is principally entropy-driven, and the enthalpy is endothermic nature for the system, the hydrophobic forces acting a significant role in the reaction. Also, the negative value of ΔG^0 means that APR binding to BSA is spontaneous. Changes in the microenvironment near Tyr and Trp residues of the protein was monitored as a result of APR binding to BSA. According to the drug displacement and molecular docking analysis, APR exhibited a stronger binding affinity towards DS2 compared to DS1.

Declaration of competing interest

The authors declare that they have no known competing financial interests or personal relationships that could have appeared to influence the work reported in this paper.

Data availability

The authors do not have permission to share data.

Acknowledgment

Ipek Kucuk thanks to the financial support from The Scientific and Technological Research Council of Türkiye (TUBITAK) under the BIDEB/2211-A doctoral scholarship program. The numerical calculations reported in this paper were partially performed at TUBITAK ULAKBIM, High Performance and Grid Computing Center (TRUBA resources).

Appendix A. Supplementary data

Supplementary data to this article can be found online at https://doi.org/10.1016/j.saa.2024.125246.

References

[1] A.S. Abdelhameed, A.M. Alanazi, A.H. Bakheit, H.W. Darwish, H.A. Ghabbour, I. A. Darwısh, Fluorescence spectroscopic and molecular docking studies of the binding interaction between the new anaplastic lymphoma kinase inhibitor crizotinib and bovine serum albumin, Spectrochim. Acta Part A, Mole. Biomole. Spectrosc. 171 (2017) 174–182, https://doi.org/10.1016/j.saa.2016.08.005.
[2] A.M. Alanazi, A.S. Abdelhameed, A spectroscopic approach to investigate the molecular interactions between the newly approved irreversible ErbB blocker "Afatinib" and bovine serum albumin, PLoS One 11 (1) (2016) e0146297.
[3] H.M. Ali, M.A. El-Hashemy, Analytical investigation of the influence of ornidazole on the native protein fluorescence, Spectrochim. Acta Part A, Mole. Biomole. Spectrosc. 201 (2018) 178–184, https://doi.org/10.1016/j.saa.2018.05.003.
[4] M. Ali, H.A. Al-Lohedan, Deciphering the interaction of procaine with bovine serum albumin and elucidation of binding site: a multi spectroscopic and molecular docking study, J. Mol. Liq. 236 (2017) 232–240, https://doi.org/10.1016/j.molliq.2017.04.020.
[5] M. Azimirad, F. Javaheri-Ghezeldizaj, R. Yekta, J.E.N. Dolatabadi, M. Torbati, Mechanistic and kinetic aspects of Natamycin interaction with serum albumin using spectroscopic and molecular docking methods, Arab. J. Chem. 16 (9) (2023) 105043, https://doi.org/10.1016/j.arabjc.2023.105043.
[6] S. Bakkialakshmi, D. Chandrakala, Investigation of the fluorescence quenching of bovine serum albumin by certain substituted uracils, J. Mol. Liq. 168 (2012) 1–6, https://doi.org/10.1016/j.molliq.2012.01.018.
[7] S. Bi, T. Zhao, Y. Wang, H. Zhou, Study on the interactions of mapenterol with serum albumins using multi-spectroscopy and molecular docking, Luminescence 31 (2) (2015) 372–379, https://doi.org/10.1002/bio.2969.
[8] G. Brambilla, T. Cenci, F. Franconi, R. Galarini, A. Macrı, F. Rondoni, M. Strozzi, A. Loizzo, Clinical and pharmacological profile in a clenbuterol epidemic poisoning of contaminated beef meat in Italy, Toxicol. Lett. 114 (1–3) (2000) 47–53, https://doi.org/10.1016/s0378-4274(99)00270-2.
[9] G. Dravecz, T.Z. Jánosi, D. Beke, D.Á. Major, G. Károlyházy, J. Erostyák, K. Kamarás, Á. Gali, Identification of the binding site between bovine serum albumin and ultrasmall SiC fluorescent biomarkers, Phys. Chem. Chem. Phys./PCCP 20 (19) (2018) 13419–13429, https://doi.org/10.1039/c8cp02144a.
[10] M. Fatima, F. Nabi, R.H. Khan, A. Naeem, Investigating the binding interaction of quinoline yellow with bovine serum albumin and anti-amyloidogenic behavior of ferulic acid on QY-induced BSA fibrils, Spectrochim. Acta - Part A: Mole. Biomole. Spectrosc. 313 (2024) 1386–1425, https://doi.org/10.1016/j.saa.2024.124076.
[11] M. Feng, S. Suryoprabowo, T. Hong, L. Liu, Q. Zheng, H. Kuang, Rapid detection of clonidine and its cross-reactivity with apraclonidine in pig urine using an immunochromatographic test strip, Food Agric. Immunol. 29 (1) (2018) 821–832, https://doi.org/10.1080/09540105.2018.1460325.
[12] R.N.E. Gammal, H. Elmansi, A.A. El-Emam, F. Belal, M.E.A. Hammouda, Exploring the molecular interaction of mebendazole with bovine serum albumin using multi-spectroscopic approaches and molecular docking, Sci. Rep. 12 (1) (2022), https://doi.org/10.1038/s41598-022-15696-4.
[13] R.N.E. Gammal, H. Elmansi, A.A. El-Emam, F. Belal, P.A. Elzahhar, A.S. Belal, M.E. A. Hammouda, Insights on the in-vitro binding interaction between donepezil and bovine serum albumin, BMC Chem. 17 (1) (2023), https://doi.org/10.1186/s13065-023-00944-z.
[14] E. Gramer, S. Busche, A. Kampik, D.G. Parsons, Efficacy of apraclonidine ophthalmic solution (lopidine) in presumed silicon oil-induced glaucoma and primary open-angle glaucoma, Graefe's Arch. Clin. Exp. Ophthalmol. 233 (1) (1995) 13–20, https://doi.org/10.1007/bf00177780.
[15] K.R. Grigoryan, H.A. Shilajyan, A.L. Zatikyan, I.L. Aleksanyan, L. P. Hambardzumyan, Spectroscopic analysis of 2-(5-mercapto-1,3,4-oxadiazol-2-yl)-6-methylquinolin-4-ol binding to blood plasma albumin, Monatsh. Chem. 153 (5–6) (2022) 507–515, https://doi.org/10.1007/s00706-022-02919-7.
[16] X. Guo, X. Sun, S. Xu, Spectroscopic investigation of the interaction between riboflavin and bovine serum albumin, J. Mol. Struct. 931 (1–3) (2009) 55–59, https://doi.org/10.1016/j.molstruc.2007.06.035.
[17] C. Hao, G. Xu, Y. Feng, L. Lu, W. Sun, R. Sun, Fluorescence quenching study on the interaction of ferroferric oxide nanoparticles with bovine serum albumin, Spectrochim. Acta Part A, Mole. Biomole. Spectrosc. 184 (2017) 191–197, https://doi.org/10.1016/j.saa.2017.05.004.
[18] Y. Hu, Y. Liu, W. Jiang, R. Zhao, Q. Song-Sheng, Fluorometric investigation of the interaction of bovine serum albumin with surfactants and 6-mercaptopurine, J. Photochem. Photobiol. B Biol. 80 (3) (2005) 235–242, https://doi.org/10.1016/j.jphotobiol.2005.04.005.
[19] A. Jalan, N.S. Moyon, Molecular interactions and binding dynamics of Alpelisib with serum albumins: insights from multi-spectroscopic techniques and molecular docking, J. Biomole. Struct. Dyn./J. Biomole. Struct. Dyn. 1–17 (2023), https://doi.org/10.1080/07391102.2023.2203256.
[20] L.N. Jattinagoudar, S.T. Nandibewoor, S.A. Chimatadar, Binding of fexofenadine hydrochloride to bovine serum albumin: structural considerations by spectroscopic techniques and molecular docking, J. Biomole. Struct. Dyn./J. Biomole. Struct. Dyn. 35 (6) (2016) 1200–1214, https://doi.org/10.1080/07391102.2016.1183229.
[21] F. Javaheri-Ghezeldizaj, A.H. Jafari, M. Mahmoudpour, M. Moghadaszadeh, R. Yekta, J.E.N. Dolatabadi, Binding process evaluation of bovine serum albumin and Lawsonia inermis (henna) through spectroscopic and molecular docking approaches, J. Mol. Liq. 331 (2021) 115792, https://doi.org/10.1016/j.molliq.2021.115792.
[22] Z. Kabir, A.K. Mukarram, S.B. Mohamad, Z. Alias, S. Tayyab, Characterization of the binding of an anticancer drug, lapatinib to human serum albumin, J. Photochem. Photobiol. B Biol. 160 (2016) 229–239, https://doi.org/10.1016/j.jphotobiol.2016.04.005.
[23] Z. Kabir, J. Seng, S.B. Mohamad, M. Bilgic, B. Uslu, Exploration of the intermolecular isoproturon–bovine serum albumin combination: biophysical and computational prospects, J. Photochem. Photobiol. A Chem. 450 (2024) 115464, https://doi.org/10.1016/j.jphotochem.2024.115464.
[24] M.Z. Kabir, J. Seng, S.B. Mohamad, B. Uslu, Decoding the intermolecular recognition mode of a potent anticancer drug, abiraterone with human serum albumin: assessments through spectroscopic and computational techniques, J. Mol. Struct. 1302 (2024) 137509, https://doi.org/10.1016/j.molstruc.2024.137509.

[25] L. Kaur, A. Singh, A. Datta, H. Ojha, Multispectroscopic studies of binding interaction of phosmet with bovine hemoglobin, Spectrochim. Acta A Mol. Biomol. Spectrosc. 296 (2023) 122630, https://doi.org/10.1016/j.saa.2023.122630.
[26] S.F. Koly, S. Kundu, S. Kabir, M.S. Amran, M.Z. Sultan, Analysis of aceclofenac and bovine serum albumin interaction using fluorescence quenching method for predictive, preventive, and personalized medicine, EPMA J. 6 (1) (2015), https://doi.org/10.1186/s13167-015-0047-x.
[27] J.R. Lakowicz, Principles of fluorescence spectroscopy, Springer eBooks (1999), https://doi.org/10.1007/978-1-4757-3061-6.
[28] K. Lindorff-Larsen, et al., Improved side-chain torsion potentials for the Amber ff99SB protein force field, Proteins 78 (8) (2010) 1950–1958.
[29] Y. Liu, M. Chen, Z. Luo, J. Lin, L. Song, Investigation on the site-selective binding of bovine serum albumin by erlotinib hydrochloride, J. Biomole. Struct. Dyn./J. Biomole. Struct. Dyn. 31 (10) (2013) 1160–1174, https://doi.org/10.1080/07391102.2012.726532.
[30] F. Macii, T. Biver, Spectrofluorimetric analysis of the binding of a target molecule to serum albumin: tricky aspects and tips, J. Inorg. Biochem. 216 (2021) 111305, https://doi.org/10.1016/j.jinorgbio.2020.111305.
[31] S. Maleki, G. Dehghan, L. Sadeghi, S. Rashtbari, M. Iranshahi, N. Sheibani, Surface plasmon resonance, fluorescence, and molecular docking studies of bovine serum albumin interactions with natural coumarin diversin, Spectrochim. Acta A Mol. Biomol. Spectrosc. 230 (2020) 118063, https://doi.org/10.1016/j.saa.2020.118063.
[32] N. Ngueanngam, B. Jityuti, S. Patnin, P. Boonsri, A. Makarasen, A. Buranaprapuk, Multiple spectroscopic and computational studies on binding interaction of 2-phenylamino-4-phenoxyquinoline derivatives with bovine serum albumin, Spectrochim. Acta A Mol. Biomol. Spectrosc. 310 (2024) 123948, https://doi.org/10.1016/j.saa.2024.123948.
[33] S.K. Pawar, J. Seetharamappa, Interaction of repaglinide with bovine serum albumin: spectroscopic and molecular docking approaches, J. Pharmaceut. Anal./J. Pharmaceut. Anal. 9 (4) (2019) 274–283, https://doi.org/10.1016/j.jpha.2019.03.007.
[34] E. Plaksej, A. Dolata, K. Wiglusz, The effect of glycation on bovine serum albumin conformation and ligand binding properties with regard to gliclazide, Spectrochim. Acta - Part A: Mole. Biomole. Spectrosc. 189 (2018), https://doi.org/10.1016/j.saa.2017.08.071.
[35] X. Qi, D. Xu, J. Zhu, S. Wang, J. Peng, W. Gao, Y. Cao, Studying the interaction mechanism between bovine serum albumin and lutein dipalmitate: Multi-spectroscopic and molecular docking techniques, Food Hydrocoll. 113 (2021) 106513, https://doi.org/10.1016/j.foodhyd.2020.106513.
[36] N. Rahman, N. Khalil, Effect of glycation of bovine serum albumin on the interaction with xanthine oxidase inhibitor allopurinol: Spectroscopic studies and molecular modeling, J. Mol. Liq. 367 (2022) 120396, https://doi.org/10.1016/j.molliq.2022.120396.
[37] P.D. Ross, S. Subramanian, Thermodynamics of protein association reactions: forces contributing to stability, Biochemistry 20 (11) (1981) 3096–3102, https://doi.org/10.1021/bi00514a017.
[38] P. Sengupta, P.S. Sardar, P. Roy, S. Dasgupta, A. Bose, Investigation on the interaction of Rutin with serum albumins: insights from spectroscopic and molecular docking techniques, J. Photochem. Photobiol. B, Biol. 183 (2018) 101–110, https://doi.org/10.1016/j.jphotobiol.2018.04.019.
[39] B. Sekula, K. Zielinski, A. Bujacz, Crystallographic studies of the complexes of bovine and equine serum albumin with 3,5-diiodosalicylic acid, Int. J. Biol. Macromol. 60 (2013) 316–324.
[40] J. Shi, Q. Wang, D. Pan, T. Liu, M. Jiang, Characterization of interactions of simvastatin, pravastatin, fluvastatin, and pitavastatin with bovine serum albumin: multiple spectroscopic and molecular docking, J. Biomole. Struct. Dyn./J. Biomole. Struct. Dyn. 35 (7) (2016) 1529–1546, https://doi.org/10.1080/07391102.2016.1188416.
[41] D. Sood, N. Kumar, G. Rathee, A. Singh, V. Tomar, R. Chandra, Mechanistic interaction study of bromo-noscapine with bovine serum albumin employing spectroscopic and chemoinformatics approaches, Sci. Rep. 8 (1) (2018), https://doi.org/10.1038/s41598-018-35384-6.
[42] D. Stan, I. Matei, C. Mihailescu, M. Savin, M. Hillebrand, I. Baciu, M. Matache, Spectroscopic investigations of the binding interaction of a new indanedione derivative with human and bovine serum albumins, Mole./Mole. Online/Mole. Ann. 14 (4) (2009) 1614–1626, https://doi.org/10.3390/molecules14041614.
[43] J. Steinhardt, J. Krijn, J.G. Leidy, Differences between bovine and human serum albumins. Binding isotherms, optical rotatory dispersion, viscosity, hydrogen ion titration, and fluorescence effects, Biochemistry 10 (22) (1971) 4005–4015, https://doi.org/10.1021/bi00798a001.
[44] N. Tayeh, T. Rungassamy, J.R. Albani, Fluorescence spectral resolution of tryptophan residues in bovine and human serum albumins, J. Pharm. Biomed. Anal. 50 (2) (2009) 107–116, https://doi.org/10.1016/j.jpba.2009.03.015.
[45] M. Toprak, M. Arık, The investigation of the interaction between orientin and bovine serum albumin by spectroscopic analysis, Luminescence 29 (7) (2013) 805–809, https://doi.org/10.1002/bio.2624.
[46] J. Wang, L. Ma, Y. Zhang, T. Jiang, Investigation of the interaction of deltamethrin (DM) with human serum albumin by multi-spectroscopic method, J. Mol. Struct. 1129 (2017) 160–168, https://doi.org/10.1016/j.molstruc.2016.09.061.
[47] B. Wang, D. Pan, K. Zhou, Y. Lou, J. Shi, Multi-spectroscopic approaches and molecular simulation research of the intermolecular interaction between the angiotensin-converting enzyme inhibitor (ACE inhibitor) benazepril and bovine serum albumin (BSA), Spectrochim. Acta Part A, Mole. Biomole. Spectrosc. 212 (2019) 15–24, https://doi.org/10.1016/j.saa.2018.12.040.
[48] T.A. Wani, A.H. Bakheit, S. Zargar, M.A. Bhat, A.A. Al-Majed, Molecular docking and experimental investigation of new indole derivative cyclooxygenase inhibitor to probe its binding mechanism with bovine serum albumin, Bioorg. Chem. 89 (2019) 103010, https://doi.org/10.1016/j.bioorg.2019.103010.
[49] T.A. Wani, A.H. Bakheit, M.N. Ansari, A.A. Al-Majed, B.M. AlQahtani, S. Zargar, Spectroscopic and molecular modeling studies of binding interaction between bovine serum albumin and roflumilast, Drug Des. Devel. Ther. 12 (2018) 2627–2634, https://doi.org/10.2147/dddt.s169697.
[50] Q. Yue, T. Shen, C. Wang, C. Gao, J. Liu, Study on the interaction of bovine serum albumin with ceftriaxone and the inhibition effect of zinc (II), Int. J. Spectrosc. 2012 (2012) 1–9, https://doi.org/10.1155/2012/284173.
[51] W. Xu, Y. Ning, S. Cao, G. Wu, H. Sun, L. Chai, S. Wu, J. Li, D. Luo, Insight into the interaction between tannin acid and bovine serum albumin from a spectroscopic and molecular docking perspective, RSC Adv. 13 (16) (2023) 10592–10599, https://doi.org/10.1039/d3ra00375b.
[52] H. Xu, Q. Liu, Y. Wen, Spectroscopic studies on the interaction between nicotinamide and bovine serum albumin, Spectrochim. Acta. Part A, Mole. Biomole. Spectrosc. 71 (3) (2008) 984–988, https://doi.org/10.1016/j.saa.2008.02.021.
[53] X. Zhang, L. Li, Z. Xu, Z. Liang, J. Su, J. Huang, B. Li, Investigation of the interaction of Naringin palmitate with bovine serum albumin: spectroscopic analysis and molecular docking, PLoS One 8 (3) (2013) e59106.